2011 7th US National Combustion Meeting
Organized by the Eastern States Section of the Combustion Institute
and Hosted by the Georgia Institute of Technology, Atlanta, GA
March 20-23, 2011

Effect of Gap Height on Thin Fuel Opposed Flow Flame Spread in the Narrow Channel Apparatus

G.W. Sidebotham[1], S.L. Olson[2], P. Rachow[3], F. J. Miller[4] and I. S. Wichman[5]

[1]Mechanical Engineering Department, The Cooper Union for the Advancement of Science and Art, New York, NY 10003, USA

[2]NASA Glenn Research Center at Lewis Field, Cleveland, OH 44135

[3]Ohio Northern University, Ada, OH, 45810

[4]Department of Mechanical Engineering, San Diego State University, San Diego, CA 92182-1323

[5]Department of Mechanical Engineering, Michigan State University, East Lansing, MI 48824-1226

The Narrow Channel Apparatus (NCA) is designed to establish a fully developed laminar flow profile above and below a thin, flat, solid fuel or on one side of a thick fuel for flame spread investigations. Due in part to its ability to suppress buoyantly-induced flow, the NCA is under investigation as a possible test method for screening materials for space flight applications. This study focused on characterizing the flame response over a range of channel gap widths and opposed air flow velocities. A key objective is to determine whether the gap width can be chosen to suppress buoyancy without excessive heat loss to the inert top and bottom plates. Tests were conducted with Whatman 44 filter paper for full gap heights between the two inert plates ranging from 6 to 20 mm (with a half-gap below and above the sample). Average opposed flow velocities ranged from 1.0 to 40 cm/s. Flame spread rates measured from video analysis ranged from 0.12 to 0.37 cm/s. Side view images were used to qualitatively assess the role of buoyancy on the flame shape. A scaling analysis shows that flames at low flows become fuel rich when the forced flow becomes of the same magnitude as diffusive flow. Heat loss increases as the quenching distance increases relative to the gap height at low flow, increasing conductive loss to the confining walls. Buoyancy suppression is achieved by making the gap as narrow as possible. For thin fuels, the data suggest that a full gap of 10 mm (half-gap of 5 mm) provides a reasonable compromise between heat loss and buoyancy suppression.

1. Introduction

Material flammability for spacecraft applications is currently evaluated using NASA-STD-6001, [1]. For non-metallic solids, the main flammability test is Test 1, Upward Flame Propagation. Induced buoyant flows generated in Test 1 are generally much larger than those found in spacecraft environments [2]. Therefore, there is an incentive to develop ground-based tests that can give information about the behavior of fires relevant to spacecraft ventilation flow rates and atmospheres.

Recent studies of flame spread over thin and thick fuels [3, 4, 5] indicate that the induced buoyant flows can be reduced by spatially confining the flow in the vertical direction. A method to do so, currently called the Narrow Channel Apparatus (NCA, shown schematically in Figure 1), has been under development for fundamental flame spread research efforts [3, 6]. Flames in the NCA appear visually similar to those that have been studied in microgravity, and exhibit similar spread rates to actual microgravity flames for very thin fuels where direct comparisons are possible [4, 5, 7]. Phenomena such as flame fingering and a low flow quenching limit have been demonstrated in the NCA that are characteristic of microgravity flames, and never observed in Test 1 [3, 6, 7]. A major concern with the NCA is the effect of flame quenching due to heat loss to the plates that confine the flow (see Figure 1). The goal of the present study is to evaluate the roles of gap height and opposed flow velocity in the NCA. Evidence of a trade-off between buoyant suppression and flame quenching is of particular interest as support for further development of a standard test method.

2. Experimental

The configuration of the NCA at NASA used for this study (Figure 1) has been described elsewhere [3, 4]. In the configuration used for this study, facility air is regulated, filtered and dried prior to entering a mass flow controller. The flow enters an inlet plenum section that conditions the flow to become fully developed laminar flow between flat plates. The test section is 38 cm wide by 45 cm long, with a total gap height (2h + t) that can be adjusted over the range of approximately 3 to 20 mm. A 0.8 mm thick stainless steel sample holder plate is placed in the center of the test section, with flow on both sides. A 5 cm by 25 cm rectangular slot is cut in the center of the sample holder to accept fuel samples (Whatman 44 filter paper). The desired air flow is established and an igniter wire placed at the trailing edge of the sample is activated, igniting a flame that propagates upstream (to the left in Figure 1) toward the supply air. The experiment is videotaped from two cameras. A top view is used to analyze the flame propagation, a side view to investigate flame shape and structure. The videos are analyzed using Spotlight software developed at NASA Glenn [8].

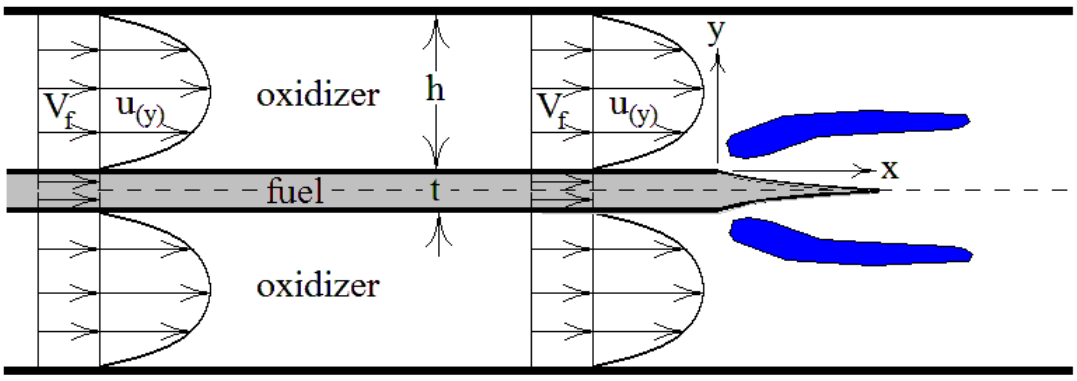

Figure 1: Schematic of the flow geometry of the Narrow Channel Apparatus for opposed flow flame spread over a thin fuel in flame fixed coordinates. The gap thickness 2h ranges from 3 to 20 mm, neglecting the fuel thickness t. V_f is exaggerated compared to $u_{(y)}$ for clarity.

3. Spread Rates and Flame Images

Figure 2 shows the flame spread rate as a function of opposed flow velocity for four gap heights. For each gap height, there is a velocity that maximizes the flame spread rate. For the two lower gap heights tests (h = 3 and 5 mm), lower opposed flows than those indicated by the left-most data points did not support a steady flame. Equipment limitations prevented an upper flow (blow off) limit to be reached except for a gap of 3 mm, in which case a test at 40 cm/s opposed flow did not yield a flame. Figure 3 shows side view images as a function of gap height and opposed flow velocity. The asymmetries between the top and bottom flames allow a qualitative assessment of buoyant effects, which tend to steepen the flame angle and change the concavity for the top flame compared to the bottom. A more detailed analysis is needed, but buoyant effects appear minor for the gap height h = 3 and 5 mm.

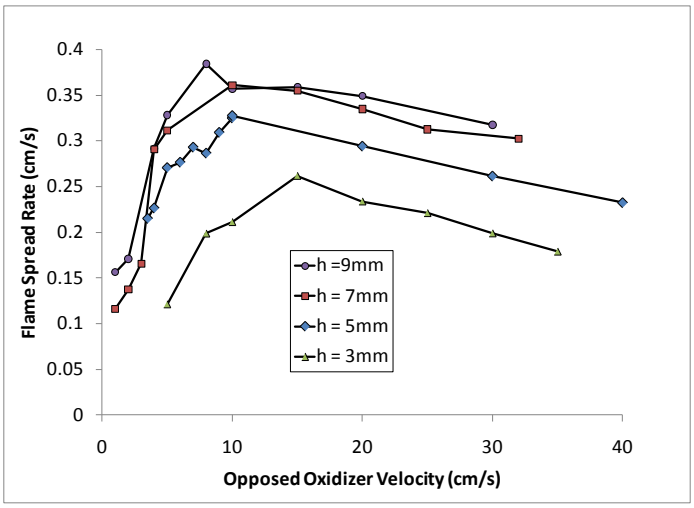

Figure 2: Flame spread rate vs opposed flow velocity

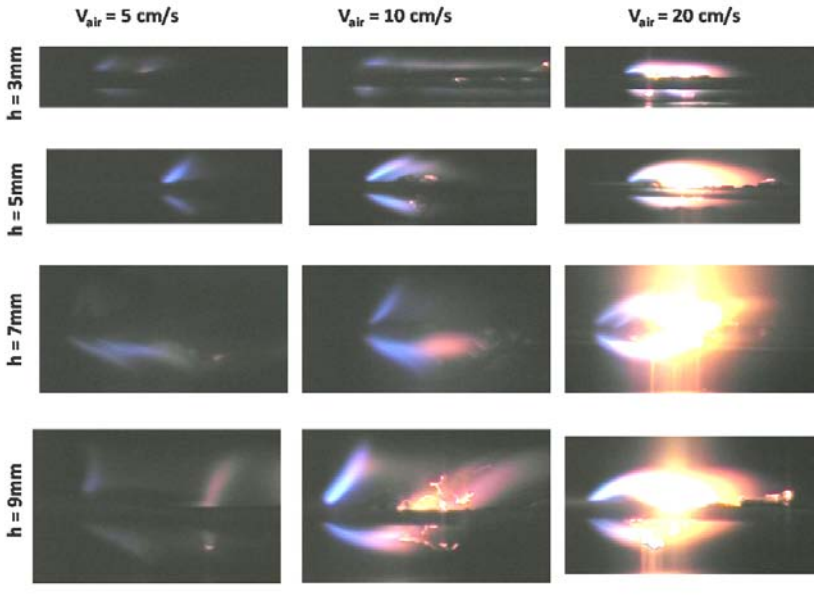

Figure 3: Side view flame images at various air velocities and gap heights. Camera settings were identical for every test, so that relative flame brightness can be judged.

4. Flame Scaling

The overall stoichiometry of a flame spreading in a narrow channel is well defined, unlike that of a flame in an open environment whose fuel lean stoichiometry has little meaning. The mass feed rates of fuel and oxidizer in flame coordinates are

$$\dot{m}_{fuel} = \rho_f V_f t_f w \qquad (1)$$

$$\dot{m}_{ox} = 2\rho_{ox}\left(V_f + V_{0x}\right)hw \qquad (2)$$

where ρ_f is the fuel density, ρ_{ox} is the oxidizer (air) density, t_f is the fuel thickness, V_f is the flame velocity, V_{ox} is the average oxidizer flow velocity and w is the sample width. The factor '2' for the oxidizer flow is due to the symmetry (flow on both sides). After rearrangement, the overall flame equivalence ratio (fuel to oxidizer feed ratio normalized by its stoichiometric value) can be expressed in terms of several dimensionless quantities:

$$\phi = \left(\frac{\rho_f}{\rho_{ox}}\right)\left(\frac{t_f}{2h}\right)\left(\frac{V_f}{V_f + V_{ox}}\right)\frac{1}{\left(F/Ox\right)_{mass,stoich}} \qquad (3)$$

The fuel to oxidizer stoichiometric mass ratio is 0.196 for cellulose ($C_6H_{10}O_5$) in air.

In the gas phase, a characteristic preheat length (δ_{gas}) can be defined by $\delta_{gas} \sim \alpha_g / V_r$ where $\alpha_g = k_g/(\rho_{ox}c_{p,g})$ is the thermal diffusivity of the gas mixture and V_r is the relative velocity seen by the leading edge of the flame which stands off from the fuel surface. In flame coordinates, with the origin placed on the wall (Figure 1), the relative velocity distribution in the upper channel for fully developed laminar flow is:

$$u(y) = V_f + 6V_{ox}\left(\frac{y}{h}\right)\left(1 - \frac{y}{h}\right) \qquad (4)$$

.

The relative velocity is taken to be the velocity seen by the flame at the quenching distance, assumed here to be equal to the gas preheat length due to the elliptic nature of the leading edge. Substituting for the preheat length:

$$\delta_{gas} \sim \frac{\alpha_g}{V_f + \dfrac{6V_{ox}\delta_{gas}}{h}\left(1 - \dfrac{\delta_{gas}}{h}\right)} \qquad (5)$$

Expanding and rearranging (with a proportionality constant of unity) yields a cubic equation for the gas preheat length:

$$\left(\frac{\delta_{gas}}{h}\right)^3 - \left(\frac{\delta_{gas}}{h}\right)^2 - \frac{1}{6}\left(\frac{V_f}{V_{ox}}\right)\left(\frac{\delta_{gas}}{h}\right) + \frac{1}{6}\left(\frac{\alpha_g}{V_{ox}h}\right) = 0 \qquad (6)$$

A closed form solution for this cubic equation is cumbersome, but it can be solved numerically, using Newton's method. This value is used in subsequent plots. However, the following simple closed form solution reveals underlying physics. If it is assumed that the gas phase preheat length is small compared to the gap height (this approximation is equivalent to assuming a constant velocity gradient, neglecting the curvature in the velocity profile, and the cubic term drops) and if the flame spread rate is assumed to be small compared to the opposed flow velocity at the quenching distance (the 3rd term drops). The largest value of the ratio of the 3rd term to the

2^{nd} of Eqn. (6) is 0.13 (for the test with h = 9 mm, V_{ox} = 5 cm/s). The gas phase preheat length simplifies to:

$$\delta_{gas} \approx \sqrt{\frac{\alpha_g h}{6V_{ox}}} \qquad (7)$$

The opposed flow velocity can be normalized by a diffusion velocity of oxygen [9], defined as $V_{ox,diffusion} \sim D_{O2} / \delta_{gas}$ where D_{O2} is the diffusion coefficient of oxidizing species (O_2) into the nominal gas mixture. A dimensionless opposed flow velocity is therefore:

$$\hat{V}_{ox} = \left(\frac{\delta_{gas} V_{ox}}{\alpha_g} \right) \left(\frac{\alpha_g}{D_{O2}} \right) \qquad (8)$$

where the Lewis number, $Le = \alpha/D$ has been introduced. Substituting for the constant gradient, low spread rate model for gas preheat length:

$$\hat{V}_{ox} \approx Le \sqrt{\frac{V_{ox} h}{6\alpha_g}} \qquad (9)$$

The dimensionless opposed flow velocity therefore has the functionality:

$$\hat{V}_{ox} = C * Le * Pe^{0.5} \qquad (10)$$

where $Pe = Vh/\alpha$ is a Peclet number. A variant of Eqns. (9) and (10) was originally derived using a theoretical analysis of the spread of a flame into a linear velocity gradient flow [10]. This analysis utilized the Wiener-Hopf technique to produce the proportionality indicated here while also generating a correlation describing flame spread finite-rate chemistry influences. The paper by Wichman, Williams and Glassman [11] examined the consequences of this model for flame spread correlations. The theoretical analysis developed here does not utilize the governing equations but uses concepts of physical modeling to develop the more general formula of Eqn. (6) which is simplified for linear velocity gradient flows to produce Eqn. (10), which, as mentioned, is also the consequence of a rigorous analysis [10, 11].

A dimensionless heat loss is defined as the ratio of the approximate heat loss (from the leading edge of the flame to the two far walls) normalized by the heat release rate:

$$\hat{Q}_{Loss} = \frac{2k_{gas} w \delta_{gas} \dfrac{T_f - T_\infty}{h - \delta_{gas}}}{\rho_{fuel} t w V_f \Delta h_c} \qquad (11)$$

The heat of combustion can be related to the flame temperature as $\Delta h_c = c_{p,gas}(T_f - T_\infty)$. This expression assumes the heat loss and the energy to vaporize the solid are negligible in comparison to the energy to raise the product gas to the flame temperature. The dimensionless heat release becomes:

$$\hat{Q}_{Loss} = \frac{2k_{gas}\delta_{gas}}{c_{p,gas}\rho_{fuel} t V_f \left(h - \delta_{gas}\right)} \qquad (12)$$

Figure 4 shows the overall flame equivalence ratio (left) and dimensionless heat loss (right) plotted against dimensionless opposed flow velocity. In both cases, the smallest gap height deviates significantly from the other curves. Overall fuel rich flames are demonstrated at sufficiently low oxidizer flows. As flow velocity is reduced and the low flow quenching limit is approached, the heat loss increases sharply.

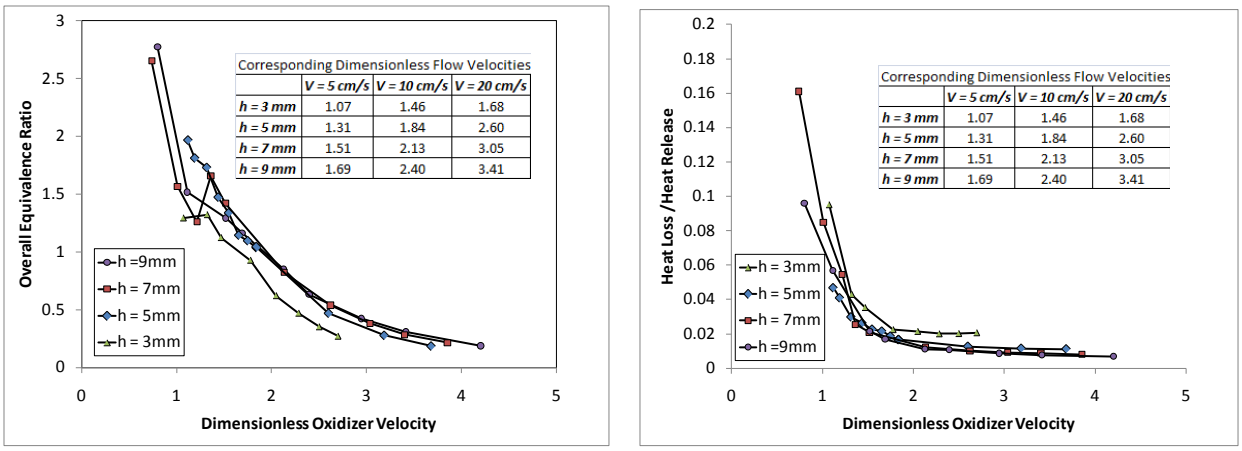

Figure 2: Overall flame equivalence ratio (left, Eqn. 3 against 8) and dimensionless heat loss (right, Eqn. 12 against 8) versus dimensionless opposed flow velocity

5. Concluding Remarks

A scaling analysis shows that flames at low flows become fuel rich when the forced flow becomes of comparable magnitude as the diffusive flow. Heat loss increases as the quenching distance increases relative to the gap height at low flow, increasing conductive loss to the confining walls. The theory leading to Eqs. (9) and (10) produces results that are in agreement with previous modeling efforts [10, 11]. This agreement is encouraging, since flame spread in spatially variable velocity fields is a topic of research that is relatively unexplored.

Buoyancy suppression is achieved by making the gap as narrow as possible. For very narrow gaps the concavity of the top-side flame is less apparent, indicating that buoyancy is suppressed. However, a narrow gap increases heat losses as seen in Figure 4 (right side, where the 3 mm data has higher non-dimensional heat losses than the other gap spacings). Of the gap heights investigated, a gap height h = 5 mm between fuel and confining wall appears to yield the best compromise between buoyancy suppression and wall heat loss in the Narrow Channel Apparatus.

Acknowledgements

Support was provided by the 2010 NASA-Glenn Faculty Fellowship Program and NASA Cooperative Agreements NNX10AD96A and NNX10AD97A.

References

[1] D.R. Mulville, NASA-STD-6001, 1998.

[2] K.E. Lange, A.T. Perka, B.E. Duffield, F.F. Jeng, NASA CR-2005-213689, 2005.

[3] F.J. Miller, S.L. Olson, S.A Gokoglu and P.V. Ferkul, *5th US Combustion Meeting, University of California at San Diego*, March 25-28, 2007.

[4] S.L. Olson, F.J. Miller, S. Jahangirian, I.S. Wichman, *Combustion and Flame*, vol. 156, 2009.

[5] G.W. Sidebotham, S.L. Olson, *Combustion and Flame*, vol. 154, #4, 2008.

[6] S.L. Olson, F.J. Miller, I.S. Wichman, *Fourth International Symposium on Scale Modeling*, Sept. 17-19, 2003.

[7] S.L. Olson, NASA TM 100195, 1987.

[8] R. Klimek, T. Wright *"Spotlight-8 Image Software Analysis"*, available at http://microgravity.grc.nasa.gov/spotlight/

[9] S.L.Olson, H.R. Baum, T. Kashiwagi, *27th Symposium (International) on Combustion*, 1998, pp.2525-2533.

[10] I.S.Wichman, *Combustion and Flame***,** Vol. 50, pp. 287-304 (1983).

[11] I.S.Wichman, F.A. Williams, I. Glassman, *19th Symposium (International) on Combustion*, pp. 835-845 (1983).